Impedancemetry of Ag$_2$S nanocrystallites embedded in nanoporous glasses

© *A.V. Ilinskiy*[1], *R.A. Castro*[2], *M.E. Pashkevich*[3], *I.O. Popova*[2], *A.I. Sidorov*[4], *E.B. Shadrin*[1]

[1] Ioffe Institute,
St. Petersburg, Russia
[2] Herzen State Pedagogical University of Russia,
St. Petersburg, Russia
[3] Peter the Great Saint-Petersburg Polytechnic University,
St. Petersburg, Russia
[4] ITMO University,
St. Petersburg, Russia

E-mail: shadr.solid@mail.ioffe.ru

The temperature dependences of the dielectric spectra of Ag$_2$S nanocrystallites synthesized inside the channels of nanoporous glasses NPG-17 with an average diameter of filamentous pores of 17 nm are studied. The macroscopic mechanism for the occurrence of the frequency dependence of the electrical response of a nanoporous structure NPG-17 + Ag$_2$S is proposed. Formation of the model of mechanism is based superionic phase transition in Ag$_2$S nanocrystallites fixed inside the channels of nanoporous glass is discussed.

Keywords: silver sulfide, Ag$_2$S, nanoporous glasses, nanostructured materials, impedancemetry.

1. Introduction

Silver sulphide is a superionic with two types of phase transitions (PT), since it exists in three crystal modifications: α (monoclinic syngony, spatial group $P2_1/c$), β (cubic syngony, spatial group $Im3m$) and γ (cubic syngony, spatial group $Pn3$) [1]. PT temperatures in volume monocrystal: 176°C for $\alpha \rightarrow \beta$ transition and 592°C for $\beta \rightarrow \gamma$. Ag$_2$S crystal structure has one interesting feature: lattice cell volume at superionic PT ($\alpha \rightarrow \beta$) reduces almost in half.

Ag$_2$S crystal structure features cause its unusual properties, study of which is of interest from both fundamental and application point of views. As it turned out, Ag$_2$S nanocrystals are resistant to mechanical deformations and complex profile pressure action due to their surface tension [2], contributing to formation of mini-supercondensers with ultrahigh density of energy, concentrated in them [3]. Fundamental study of „semiconductor-superionic" PT in Ag$_2$S nanocrystals is also relevant, since superionic PT in nanoelement starts from high-temperature superionic phase formation on its surface. With temperature increase the phase boundary slowly moves inside nanoelement, while physical mechanism of size dependence of PT parameters remains unknown [4]. Another aspect of superionics application, which are also called solid electrolytes: superionic materials are widely used as a working medium with combined electron-ionic conductivity [5].

Interesting results of superionics study are observed using dielectric spectroscopy (DS) method, that is often called impedance spectroscopy in literature [6]. This method is used for studying the temperature dependencies of functional features of frequency dependencies of dielectric loss tangent and dielectric relaxators distributions by relaxation time (Gavrilyak−Negami function). Besides, the impedancemetric method allows to study size dependence of relaxation parameters of nanocrystallites of thin films [7]. A new aspect of studies using DS methods is revealed when studying Ag$_2$S nanocrystals, embedded into nanoporous glasses (NPG).

The purpose of this work is to observe the features of superconductor-superionic PT mechanism in nanocrystalline Ag$_2$S elements, fixed in NPG channels. For that purpose we studied the temperature dependencies of DS of porous glasses NPG-17 with Ag$_2$S nanocrystallites inside the channels, the numerical modeling of experimental results based on the corresponding equivalent electric schemes was performed, as well as interpretation of the observed data by calculation results comparison with experimental DS parameters.

2. Technique

2.1. Samples

NPG present a class of solid nanostructured systems. NPG were synthesized in ITMO University. Carcass of NPG-17 consists of SiO$_2$. Spatial structure is characterized by presence of through branched nanofilaments with thickness of 17 nm. Volume ratio of the filled space is 50%. Developed porous structure of glass allows to use

NPG for synthesis of Ag_2S nanocrystals, that cumulatively form thin filaments, that serves as a base for obtaining the compositional materials with size-dependent properties. Typical size of NPG samples was $10 \times 10 \times 1$ mm.

The procedure of „incremental building", providing pores filling with Ag_2S nanocrystallites, was used for NPG plates with through porosity. For that silver chlorides/nitrates were used with their further processing in hydrogen sulphide vapors with removal of the formed acid [8].

2.2. Dielectric spectroscopy

Impedancemetric measurements were performed at „Concept 81" spectrometer made by Novocontrol Technologies using „Alpha-Beta Impedance Analyzer". NPG sample with Ag_2S was put into spectrometer cell between flat gold-plated electrodes of round shape with diameter of 15 mm. Geometrical capacity of empty cell — $C_0 = 1.7$ pF. Current amplitude I_0 and phase difference φ of oscillations $U(t)$ and $I'(t)$ were measured, where $I'(t)$ is a current, flowing through the sample with application of a reference sinusoidal voltage $U(t)$ to it with amplitude of 1 V. Using the analyzer these data were converted into frequency dependencies of dielectric loss tangent tg δ and real and imaginary parts of permittivity ε. Computer programs developed by Novocontrol Technologies were used in conversion.

DS of dielectric loss tangent $tg\delta(f)$, real $\varepsilon'(f)$ and imaginary $\varepsilon''(f)$ parts of ε were made in a range from 10^{-1} Hz to 10^6 Hz. NPG sample temperature was changed in interval of $0 < T < 250°$C with a step of $10°$C.

3. Experimental results and their interpretation

3.1. Results of preliminary DS experiments with NPG samples, pores of which are filled with Ag_2S monocrystallites

The frequency dependencies of tg $\delta(f)$ for NPG samples with Ag_2S in pores were obtained at various temperatures for preliminary experiments. At $0°$C the maximum of tg δ with value $(tg\delta)_{max} \cong 0.3$ was observed at frequency of 0.1 Hz. With temperature growth the maximum, without changing its numerical value, shifted towards high frequencies and at $40°$C was located at frequency of 1 Hz. With the further temperature increase the maximum shifted in reverse direction, i.e. towards low frequencies, and at temperature of $80°$C it was back at frequency of 0.1 Hz. The further temperature increase was accompanied with formation of a new maximum, that with growth of T started to move towards high frequencies, increasing in value from 0 to tg $\delta = 2$ at $f = 7$ Hz and $T = 250°$C. With the further temperature decrease back to $0°$C the value of tg δ was less than the initial value (tg $\delta \cong 0.01$) by an order, and DS was largely widened, differing by shape from initial DS of tg $\delta(f)$ as a clear maximum. Such complex temperature

changes of DS in a region of $T = 40-50°$C, far from T_c of PT ($176.3°$C) in Ag_2S, resulted in conclusion, that DS features of NPG + Ag_2S can be significantly distorted by influence of some external factor. The most probable cause of distortions is influence of water, penetrating the glass pores due to atmospheric action [9].

Due to possibility of atmospheric moisture adsorption inside NPG pores, that could cause the distortion of the experimental results, we performed control DS studies of NPG samples with pores, filled with water in advance. After that we performed studies of the sample with pores, filled with Ag_2S monocrystals, but with pre-dehydration with heating.

## 3.2. Results of control DS experiments with NPG samples, pores of which are filled with water

NPG samples, pores of which were filled with distilled deionized water, were used in the experiments. Figure 1 shows DS of these samples: frequency dependencies of dielectric loss tangent tg $\delta(f)$ at various temperatures. At $0°$C the maximum of tg δ with value $\cong 1$ was observed at frequency of 9 Hz. With temperature growth the maximum, without changing its numerical value, shifted towards high frequencies and at $50°$C was located at frequency of 100 Hz. With the further temperature increase the maximum shifted in reverse direction, i.e. towards low frequencies, and at temperature of $110°$C it went beyond operating frequency range of dielectric spectrometer. With the repeated temperature reduction to $0°$C the described maximum was not observed.

Mathematical modeling. Single-loop scheme is applied — insert in Fig. 1. It includes two successive capacities: NPG sample capacity — C_I and its electrode sheath capacity C_{II}. Leak resistance, modeling ohmic resistance of water, filling the glass pores, is connected parallel to the sample capacity. Frequency dependence of tg $\delta(\omega)$ in single-loop scheme is derived from expression [10]:

$$tg\,\delta(\omega) = (R_I\omega C_{II})/[1 + R_I^2\omega^2 C_I(C_I + C_{II})], \quad \omega = 2\pi f.$$

By setting the function frequency derivative tg $\delta(f)$ to zero, we obtain, that position of the maximum on frequency axis f_{max} is in linear dependence on electrical conductivity of water $1/R_I$, filling the pores ($f_{max} \sim 1/R_I$). With increase of R_I the maximum shifts towards high frequencies, and with increase of R_I — towards low frequencies.

Interpretation. Electrical conductivity of liquid distilled water has ionic nature, and with temperature growth the mobility of ions increases due to thermal loosening of structure of spatial hydration sheaths of oxygen ions, formed based on hydrogen bonds. This defines thermal reduction of low-frequency ohmic resistance R_I of the sample. At $50°$C destruction of spatial structure of the sheaths completely ends, and only flat structures remain, integrity of which is also provided by hydrogen bonds, but which, however, do not prevent from initiation of the process of water intensive evaporation from the glass pores.
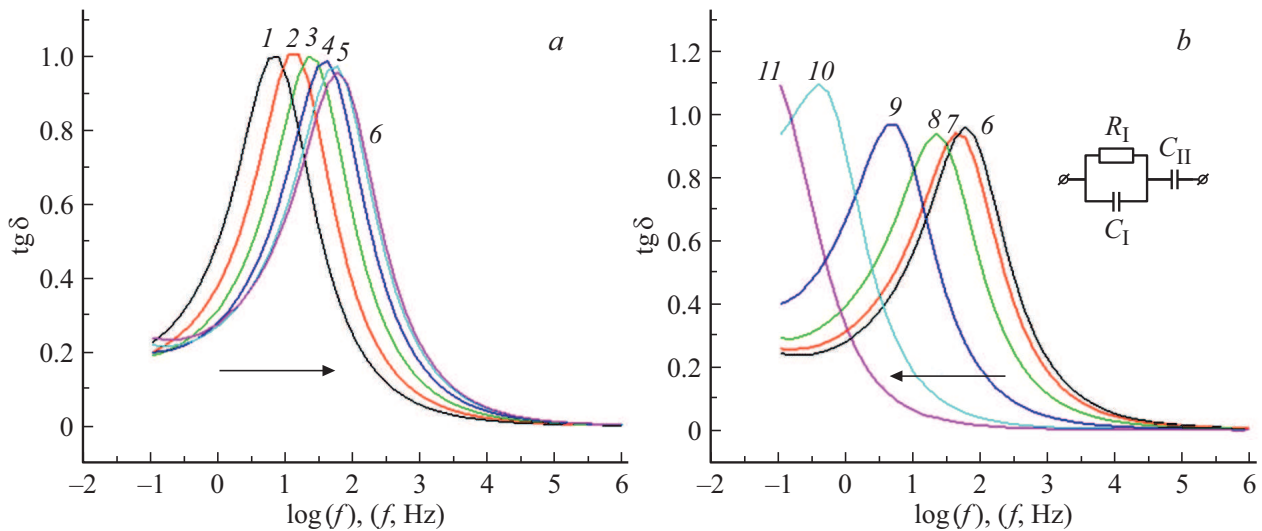
Figure 1. Frequency dependencies of tg$\delta(f)$, obtained at temperature T in a range from 0 to 100°C for NPG samples with pores, filled with water. With increase of T at first the maximum of tgδ moves towards high frequencies (right arrow (*a*)), and then at $T > 50$°C — towards low frequencies — (left arrow (*b*)). $T = 0$°C (*1*), 10°C (*2*), 20°C (*3*), 30°C (*4*), 40°C (*5*), 50°C (*6*), 60°C (*7*), 70°C(*8*), 80°C (*9*), 90°C (*10*), 100°C (*11*).

The thing is that water moistens inner surface of specially purified pores, while excessive pressure of surface tension at such a small pores diameter (17 nm) is extremely high (as per Laplace theorem). From here it follows, that at such absolute moisture the growth of saturation pressure with curve increase requires evaporation increase. Therefore, drops with small curve radius are evaporated quite intensively. Besides, the process if evaporation is additionally intensified due to growth of temperature T. Thus, the intensive water evaporation results in, starting from some temperature T_{kr}, growth of total resistance R_I of NPG sample with water in pores, since the process of total water mass loss dominates, starting from T_{kr}.

Competition of the described inversely operating factors provides in our case the minimum of function $R_I(T)$ at 50°C. With temperature increase above 50°C water intensively evaporates (PT of the first order is observed in the system), while its amount in pores quickly reduces with heating until complete disappearance. Therefore, at $T > 50$°C the significant temperature growth of resistance R_I of the sample of NPG + H$_2$O and displacement of tgδ maximum towards low frequencies are observed.

3.3. Results of DS experiments of pre-dehydrated NPG samples with pores, filled with monocrystallites of Ag$_2$S

Thus, as demonstrated by the preliminary experiments performed in this work, the nanoporous glass pores effectively adsorb the atmosphere water vapors, complicating the obtaining of information on parameters of Ag$_2$S nanocrystals, localized in the glass channels. Therefore, we

took measures to remove negative water influence on the experimental results.

NPG, in pores of which the Ag$_2$S nanocrystallites were synthesized, were used in the experiments. The samples were pre-heated to 110°C to remove water, that can penetrate the glass pores during the samples storing under laboratory conditions.

Figures 2, 3 show the frequency dependencies of tg$\delta(f)$ and Cole−Cole diagrams of $\varepsilon''(\varepsilon')$ of NPG samples with Ag$_2$S in pores. At 0°C the maximum of tg$\delta(f)$ function was observed, located at frequency of 0.5 Hz, with numerical value of tg$\delta(f_{max}) = 0.35$. With temperature growth in interval of 0−200°C the maximum monotonously shifted towards high frequencies in interval of 0.5−300 Hz, while its value gradually increases from 0.35 to 0.6. Displacement stopped at high temperatures in a range of 160−200°C. With temperature lowering the frequency positions of these maximums reproduced, thus excluding the possibility of measurement of temperature hysteresis of frequency positions.

But at high temperatures (110−250°C) in the region of low frequencies f (0.1−1 Hz) the value of tgδ significantly increased with growth of T (from value of 0.5 to 10), i.e. the slope of the second maximum of tg$\delta(f)$, which frequency position was beyond spectrometer measurement range, started to appear. With T lowering the value of tg$\delta(f)$ at frequency of 0.1 Hz was different, thus allowing to register the thermal hysteresis of tg$\delta(f)$ value.

Figure 4, *a* shows the temperature hysteresis loop with numerical value of tg$\delta(T)$ function at frequency of 0.1 Hz. The loop is located in temperature region of 160−220°C and has a width of 60°C, thus indicating the PT in this temperature region. It should be noted, that Cole−Cole
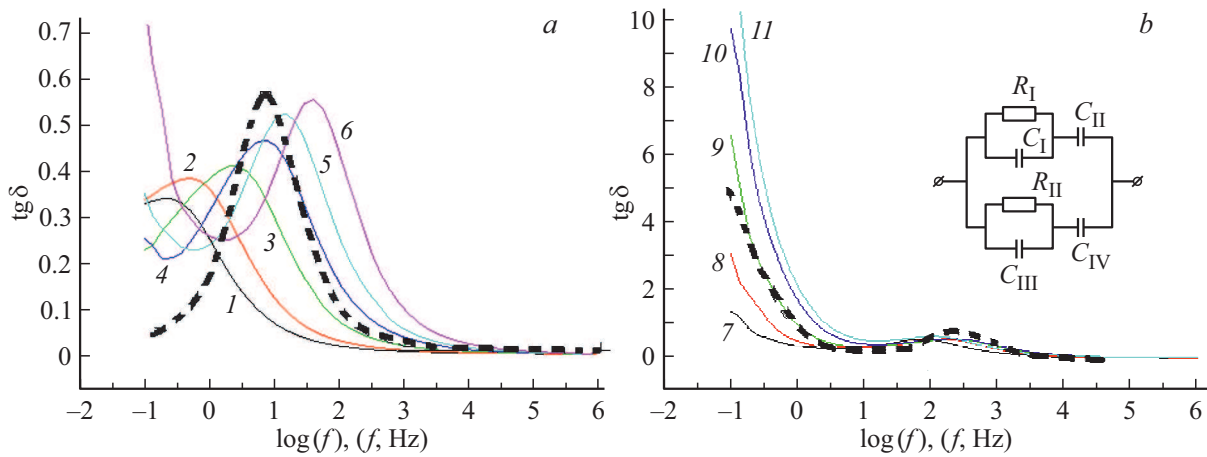
Figure 2. Frequency dependencies of $\text{tg}\,\delta(f)$, obtained at temperature T in a range from 0 to 200°C for NPG samples with pores, filled with Ag_2S. With growth of T at first the movement of $\text{tg}\,\delta$ maximum towards high frequencies (curves $1-6$ — a) is observed, and then at $T > 100$°C the second maximum of $\text{tg}\,\delta$ appears in the low frequencies regions (curves $7-11$ — b). $T = 0$°C (1), 20°C (2), 40°C (3), 60°C (4), 80°C (5), 100°C (6), 120°C (7), 140°C (8), 160°C (9), 180°C (10), 200°C (11). Dashed curves — calculation results: a — $C_I = 2\,\text{pF}$, $C_{II} = 10\,\text{pF}$, $R_I = 2 \cdot 10^9\,\Omega$, $C_{III} = 2\,\text{pF}$, $C_{IV} = 800\,\text{F}$, $R_{II} = 2 \cdot 10^{12}\,\Omega$ (dashed curve corresponds to the curve 4 at $T = 60$°C); b — $C_I = 2\,\text{pF}$, $C_{II} = 10\,\text{pF}$, $R_I = 10^8\,\Omega$, $C_{III} = 2\,\text{pF}$, $C_{IV} = 800\,\text{pF}$, $R_{II} = 2 \cdot 10^{10}\,\Omega$ (dashed curve corresponds to the curve 9 at $T = 160$°C).
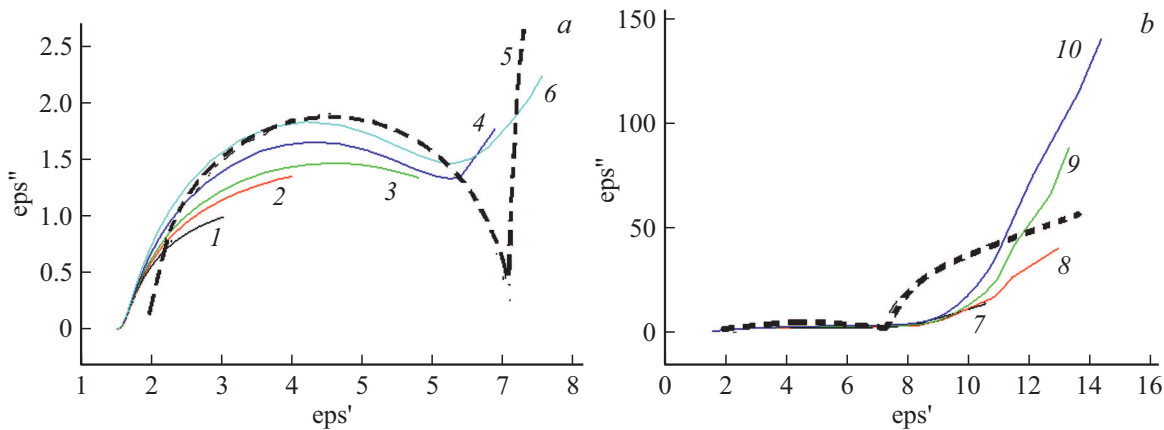
Figure 3. Cole−Cole diagrams, obtained experimentally at temperature T in a range from 0 to 200°C for NPG samples with pores, filled with Ag_2S. With growth of T a semi-circle forms in the high frequencies region (curves $1-6$ — a), and then at $T > 100$°C the second semi-circle in the low frequencies regions appears (curves $7-10$ — b). $T = 0$°C (1), 20°C (2), 40°C (3), 60°C (4), 80°C (5), 100°C (6), 120°C (7), 140°C (8), 160°C (9), 180°C (10). Dashed curves — calculation results: a — $C_I = 2\,\text{pF}$, $C_{II} = 10\,\text{pF}$, $R_I = 2 \cdot 10^9\,\Omega$, $C_{III} = 2\text{pF}$, $C_{IV} = 800\,\text{pF}$, $R_{II} = 2 \cdot 10^{12}\,\Omega$ (dashed curve corresponds to the curve 4 at $T = 60$°C); b — $C_I = 2\,\text{pF}$, $C_{II} = 10\,\text{pF}$, $R_I = 10^8\,\Omega$, $C_{III} = 2\,\text{pF}$, $C_{IV} = 800\,\text{pF}$, $R_{II} = 2 \cdot 10^{10}\,\Omega$ dashed curve corresponds to the curve 9 at $T = 160$°C.

diagrams at high frequencies are almost constant in temperature region of 0−250°C (Fig. 3).

Besides, for samples of NPG + Ag_2S the temperature dependencies of characteristic time τ_{max} were obtained for relaxators, forming the Gavrilyak−Negami (GN) function — Fig. 4, b. In NPG + Ag_2S, as shown in Fig. 4, b, there are two relaxators of ionic type, since their frequencies in heating maximums of GN function are rather low (1/850 Hz and 1/300 Hz respectively). Relaxators of electron type are also observed, but their times τ_{max} are low and they are not observed in linear scale (their frequencies are beyond region of 1−100 Hz). Figure 4, b demonstrates the presence

of temperature hysteresis of Gavrilyak−Negami function features: peaks of τ_{max} on a heating curve are located higher in terms of temperature, than on a cooling curve.

Mathematical modeling. Since 2 maximums of $\text{tg}\,\delta(f)$ and 2 half-circles are observed during the experiment, for modeling we used 2-loop scheme, presented in insert in Fig. 2. Loops are connected parallel to each other. Calculations of this scheme parameters, performed using symbolic method, are presented in [10].

At low temperatures (0−110°C) all nanocrystallites of Ag_2S are in semiconductor phase, and for DS description the first loop, in which resistance R_I of Ag_2S semiconductor,
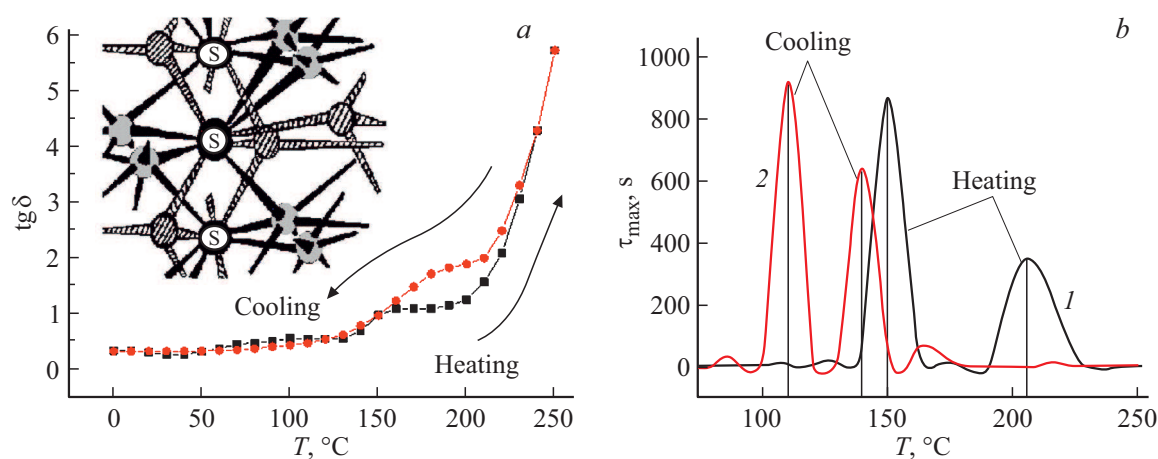
Figure 4. *a*) — temperature hysteresis of tg δ value for dehydrated samples of NPG + Ag$_2$S at frequency of $f = 0.1$ Hz, *b*) — temperature dependencies of values of characteristic relaxation time τ_{max} at heating (curve *1*) and cooling (curve *2*). Insert shows a fragment of Ag$_2$S lattice with tetracoordinate (solid circles) and octacoordinate (toned circles) ions of Ag$^+$.

filling the porous glass channels, is connected parallel to the glass capacity C_I, can be used. Capacity C_{II} is a capacity of thin dielectric layers between electrodes of dielectric spectrometer and the sample. Frequency position of the only maximum of tg δ in this case is defined exclusively by value of active resistance R_I. With increase of T the electrons are thrown to semiconductor crystallites conductivity band, resistance R_I decreases — maximum of tg $\delta(f)$ shifts towards high frequencies. The second loop, „responsible" for appearance of the second maximum of tg $\delta(f)$, is not important at this stage, since resistance R_{II} is very high.

At high temperatures (110−250°C) the superionic PT gradually happens, and for DS description initially two loops „operate" and then only the second one. Significant difference of the second loop from the first one: high values of capacity C_{IV} ($C_{IV} \gg C_{II}$) and resistance R_{II} ($R_{II} \gg R_I$). With increase of T the „free" Ag$^+$ ions appear, high resistance R_{II} decreases, the second maximum of tg $\delta(f)$ appears in DS in the low frequencies region. High value of C_{IV} we associate with formation of a thin metallic silver layer at PT in near-electrode sample regions.

Dashed lines in Figs 2, 3 indicate DS, obtained as a results of equivalent electric scheme calculation. Numerical values of the scheme parameters — capacities ans resistances — are selected for DS at temperature of 60 and 160°C and presented in the figure caption. Calculation curves are in good agreement with the experimental data.

Interpretation. Electrical conductivity of semiconductor phase of Ag$_2$S has electron nature, increasing with temperature growth. This explains the monotonous shift of „electron" maximum of tg δ towards high frequencies with the following stop at high temperatures (160−250°C), i.e. the gradual reduction of resistance R_I of nanocrystals, filling the pores, happens. However, with temperature increase the superionic PT happens at $T = T_c$: crystalline modification α-Ag$_2$S transitions into modification of β-Ag$_2$S. At the same time, the „liquid" fraction of silver ions appears,

which conductivity now has mainly ionic nature, that additionally reduces the sample resistance and exponentially increases the value of tg δ at low frequencies. It is also naturally to expect, that this PT will have temperature hysteresis. Therefore, we registered DS at increase and decrease of temperature. Figure 4, *a* shows the temperature hysteresis loop with value of tg δ at frequency of 0.1 Hz. According to this figure, PT happens in temperature region of 160−220°C, i.e. presents a superionic transition of $\alpha \rightarrow \beta$, while its properties are mainly defined with ionic, not electron conductivity of the sample. This is caused by a change of crystal lattice structure with simultaneous appearance of silver ions liquid phase in the lattice, that for the melting component of crystal structure represents PT of „order-disorder" type, at which an unordered phase is always above an ordered phase in terms of temperature. It should be noted, that the wide temperature hysteresis is characteristic for this type of transition.

Low-temperature (147°C) heating peak of τ_{max} for GN function (Fig. 4, *b*) is reasonably to associate with unmelted part of Ag$_2$S lattice, assuming, that it is caused by ionic relaxation of heavy silver ions (start of superionic PT at 150°C in nanocrystals, free from compression action of pores walls). High-temperature peak τ_{max} is associated with dielectric relaxation of silver ions of the melted (liquid) phase, since it coincides by temperature with the heating branch of hysteresis tg δ, which value for liquids is usually relatively high. Thermal hysteresis of this peak of GN function is rather wide (73°C) and presents a case of additional widening of thermal hysteresis loop due to formation of supercooled liquid inside Ag$_2$S crystal lattice.

4. Discussion

As was mentioned in introduction, silver sulphide is subjected to superionic PT from monoclinic crystal

α-modification to cubic β-modification at temperature of $T_c = 176°C$. Fig. 4,a shows the fragment of crystal lattice of Ag_2S with tetracoordinate and octacoordinate ions of Ag^+ [11].

In our work [11] we showed, that with temperature growth the bond rupture of ions of octa-Ag happens, not ions of tetra-Ag, which remain unaffected by heating. Ions of octa-Ag can move over crystal lattice as liquids with high viscosity. When reaching a critical concentration of the ruptured weaker octa-Ag-S-bonds, the crystal lattice changes its symmetry from monoclinic to cubic — structural PT with characteristic temperature hysteresis is observed. At the same time, the lattice itself remains stable due to stronger tetra-Ag-S-σ-bonds.

Low-temperature (monoclinic) phase is a direct band semiconductor with forbidden band width of $E_g = 0.9\,eV$ [12]. Energy κT, corresponding to temperature $T_c = 176°C$, is just $40\,meV$. However, rupture of octa-bonds happens due to correlation properties of Ag_2S compound. The thing is that silver atom with strong correlation properties [13] initiates ability of crystal bands to reduce its energy position at their population with electrons. Therefore, the thermal excitation of small amount of electrons into conductivity band in strongly correlated compound results in significant reduction of width of the forbidden band E_g.

From the above it follows, that the temperature-extensive (in pre-critical region) correlation reduction of E_g precedes the structural PT. It corresponds to a concept, adopted in literature, according to which the temperature-extensive correlation Mott transition [14] initiates the structural (in case of Ag_2S — superionic) PT. For the melting silver sublattice the temperature-extensive ionic PT of „order−disorder"type is also observed, and its process can be qualitatively described the following way. At $110°C$ the rupture of octa-Ag-S-bonds of a sublattice of octa-coordinate Ag^+ ions starts, while concentration of the ruptured bonds in it reaches the critical value at $160-170°C$ (the lattice is completely „melting"), resulting in structural PT of $\alpha-\beta$.

It should be noted, that electrical resistance R_{II} of NPG sample with large numerical value slightly reduces with temperature growth, while at the same time the dielectric loss tangent strongly increases with T increase. The reason for different heating action to numerical values of the specified physical quantities is the following.

In pre-critical region of temperatures $(110-150°C)$ the electrical resistance R_{II} slightly reduces in the low-frequency region due to low thermal growth of through ionic current, that is caused by low growth of concentrations of the ruptured octa-Ag-bonds and, as a result, free Ag^+ ions. At the same time, even insignificant thermal loosening of Ag-S-bonds of octa-sublattice strongly increases ability of screening of external electrical field by NPG sample at low frequencies $(0.1\,Hz-1\,Hz)$ due to thermal growth of deformation polarizability of the loosening octa-sublattice. This process does not require growth of concentration of

completely free silver ions, which is required for thorough current growth, and thermal growth of deformation polarizability of silver sublattice, preparing to melting, is sufficient. Screening ability growth results in the sample electric capacity growth. This, in its turn, is accompanied with growth of product of $R_{II}C_{IV}$ and growth of numerical value of $tg\,\delta(f)$ function. Additional confirmation of ionic nature of the described processes is a presence of extremely long relaxation times, corresponding to Gavrilyak−Negami function peaks (Fig. 4,b).

5. Conclusion

Temperature dependencies of DS of Ag_2S nanocrystals, embedded into porous glasses (NPG) with pore sizes of up to $17\,nm$, are studied in the work. Macroscopic mechanism of frequency dependence of electric response of porous structure based on Ag_2S, including equivalent electrical scheme of porous structure, is proposed. Along with macroscopic, the micromodel of thermal PT of „semiconductor-superionic" type in crystallites of Ag_2S, fixed in nanochannels of porous glass, is analyzed. Based on qualitative analysis of Ag-S-bonds energy the assumption is made, that octa-coordinate Ag ions are the main contenders for constituent elements of high-viscosity liquid, initiated with formation of the „melted" lattice part after superionic PT. During DS analysis it was established, that, quite the opposite, tetra-coordinate Ag ions are the main elements of the „unmelted" part of the crystal structure, stabilizing the crystal lattice.

It is shown, that there are three types of phase transformations in Ag_2S:

— in pre-critical region the temperature-extensive correlation electron Mott transition happens;

— in pre-critical temperature region the temperature-extensive ionic PT of „order−disorder" type happens in octa-sublattice of Ag_2S;

— at critical temperature T_c the structural superionic PT happens from α-phase to β-phase.

Dielectric spectroscopy thus allows not only to clarify the macroscopic features of electrical response of NPG with pores, filled with superionics, to oscillating electrical field exposure, but also generates a base for creation of a microscopic model of phase transformation process in superionics. DS technique, applied in this work, and information, obtained based on it, can be used for study of other materials with superionic PT, such as AgI, AgSe, AgTe or Ag_2GeS_3.

Conflict of interest

The authors declare that they have no conflict of interest.

References

[1] Zhenwei Wang, Kaifa Luo, Jianzhou Zhao, Rui Yu. Phys. Rev. B **100**, 205117 (2019).

[2] I.A. Khakhaev, F.A. Chudnovsky, E.B. Shadrin. FTT **36**, *6*, 1643 (1994) (in Russian).

[3] Z.K. Liu, J. Jiang, B. Zhou, Z.J. Wang, Y. Zhang, H.M. Weng, D. Prabhakaran, S-K. Mo, H. Peng, T. Kim, M. Hoesch, Z. Fang, X. Dai, Z.X. Shen, D.L. Feng, P. Dudin, ZY.L. Chen. Nature Mater. **13**, 677 (2014).

[4] Jun Liu, Lu Chen, Hangsheng Yang, Ze Zhang, Yong Wang. Prog. Nature Sci.: Mater. Int. **29**, 397 (2019).

[5] E.A. Ukshe, N.G. Bukun. Tverdye elektrolity. Nauka, M. (1977). 176 p. (in Russian).

[6] O. Alekperov, O. Samedov, R. Paucar, N. Abdulzade, E. Nakhmedov, A. Nadjafov, K. Wakita, N. Mamedov. Phys. Status Solidi C **12**, *6*, 610 (2015).

[7] A.S. Volkov, G.D. Koposov, R.O. Perfil'ev, A.V. Tyagunin. Optika i spektroskopiya **124**, *2*, 206 (2018) (in Russian).

[8] O.P. Vinogradova, I.E. Obyknovennaya, A.I. Sidorov, V.A. Klimov, E.B. Shadrin, S.D. Khanin, T.A. Khrushcheva. FTT **50**, *4*, 734, (2008) (in Russian).

[9] S.B. Vakhrushev, A.V. Filimonov, E.Yu. Koroleva, A.A. Naberezhnov, Yu.A. Kumzerov. Fizika nanokompozitnykh materialov. Izd-vo Politekhn. un-ta, SPb (2010). 177 p. (in Russian).

[10] A.V. Ilinskiy, R.A. Kastro, M.E. Pashkevich, E.B. Shadrin. ZhTF **89**, *12*, 1884, (2019) (in Russian).

[11] A.V. Ilinskiy, R.A. Kastro, M.E. Pashkevich, I.O. Popova, E.B. Shadrin. FTT **62**, *12*, 2138 (2020) (in Russian).

[12] D.I. Bletskan, V.V. Vakul'chak, A.V. Lukach, I.P. Studenyak. Nauch. vestn. Uzhgorodskogo un-ta. Ser. fiz. **40**, 30 (2016) (in Russian).

[13] A.S. Davydov. Kvantovaya mekhanika. Nauka, M. (1973). 703 p. (in Russian).

[14] A.V. Ilinskiy, O.E. Kvashenkina, E.B. Shadrin. FTP **45**, *9*, 1197, (2011) (in Russian).